v. 4, n. 9, 2024

Journal of Engineering Research

EFFICIENCY AND INFLUENCE OF PH, CONCENTRATION AND AERATION IN HETEROGENEOUS PHOTOCATALYSIS METHYLENE BLUE

Bruno Lellis
Student of the Postgraduation Course in Sanitation and Environment at: ``Centro Universitário de Lins`` – Unilins, Lins-SP, Brazil
http://lattes.cnpq.br/8035447206261675

Cássio Luís Fernandes de Oliveira
Advisor; Dr. Professor of the Postgraduation Course in Sanitation and Environment at: ``Centro Universitário de Lins`` – Unilins, Lins-SP, Brazil

Abstract: This article aims to verify the efficiency and influence of pH, concentration and aeration on the heterogeneous photocatalysis of methylene blue. Dyes are used massively by the global textile industry and harm water quality when discarded into bodies of water. In particular, in addition to exhibiting toxicological aspects, the methylene blue dye makes it difficult for aquatic plants to carry out photosynthesis. By employing heterogeneous photocatalysis, associating TiO2 with UV light, we sought to verify whether methylene blue can be removed from water. Factorial planning 23 and the normal probability graph showed that pH and TiO2 concentration, as well as their interaction, directly influence the process, while aeration is less significant, given the excessive formation of bubbles and low dissolved oxygen levels. Despite possible improvements to be suggested to the experiment, the photocatalytic treatment proved to be successful with 89.01% global efficiency.
Keywords: Advanced oxidative processes. Heterogeneous photocatalysis. Titanium dioxide. Methylene blue.

INTRODUCTION

Water is the most abundant compound on Earth and plays an invaluable role in transport, energy generation, irrigation, supplying cities and, above all, industrial activities. However, only 3% of the planet's water is fresh and an even smaller percentage of this substance is available in lakes and rivers. Therefore, water must be seen as vital (ROBINSON et al., 1996; SHAMMAS; WANG, 2011; LANGMUIR; BROECKER, 2012).

Water quality, however, can be compromised by natural or anthropogenic causes. In fact, the natural sources of water degradation are related, for example, to erosion, volcanism and biological processes (AGARWAL, 2009; HORNE, 2017).

On the other hand, anthropogenic sources are varied and can be concentrated, as in the case of the release of domestic and industrial waste, or dispersed, as in the intensive use of agricultural pesticides. Despite its multiple expressions, anthropogenic pollution is the decisive factor in the substantial introduction of harmful compounds into water, which will affect or compromise its quality (VON SPERLING, 2005).

The anthropogenic activity that most contributes to water contamination is, undeniably, industrial (SALLES; PELEGRINI; PELEGRINI, 2006).

In this sense, it must be noted that the industrial degradation of water quality includes the release of effluents, the dumping of solid waste in landfills located close to surface and underground water bodies, as well as the discharge of waste from mining activities (SENGUPTA, 2018).

However, it must be said that the discharge of effluents stands out as the worst form of industrial water degradation, which has grown in recent decades and has become a substantial challenge to the community and the environment (BRITO; SILVA, 2012).

The textile industry, in this context, assumes special prominence due to the large magnitude of the effluents produced, which constitute an essential issue to be addressed (KUNZ, 2002). In fact, the average water consumption for dyeing varies from 150 to 200 liters per kg of fabric, which basically depends on the type of dye used (VARANDANI, 2017).

It is not without reason, then, to note that the World Bank estimates that around 17% to 20% of industrial water pollution results from textile dyeing activities (KANT, 2012).

Due to the complexity and extent of the processes involved in the textile industry, around 3,600 textile dyes and more than 8,000 compounds are manufactured and used each

year. The result is the generation of textile effluents that exhibit a substantially diverse or heterogeneous chemical composition (ARAUJO; YOKOYAMA; TEIXEIRA, 2006; KANT, 2012; BHATIA, 2017).

Although the type of industrial processing used determines the specific characteristics of each textile effluent, it is observed that the majority results in several compounds that are considerably harmful or toxic to water quality (PATEL; VASHI, 2015).

Therefore, in addition to generating a large amount of total dissolved solids, low levels of dissolved oxygen and high chemical (COD) and biological oxygen (BOD) demands, textile effluents are one of the main responsible for the release of heavy metal cations (Cr, Ni, Cu), chlorinated organic compounds and surfactants in water bodies (ARAUJO; YOKOYAMA; TEIXEIRA, 2006; VARANDANI, 2017).

From a toxicological point of view, most dyes are poisonous or harmful to humans. Acute exposure to dyes can cause dermatological irritation, allergic conjunctivitis, rhinitis and occupational asthma. Chronic exposure, in turn, is related to carcinogenicity, as dyes and their respective metabolites can react with DNA (GREGORY, 2007; KANT, 2012).

In the case of the textile dye methylene blue (MB), its presence can cause nausea, vomiting, diarrhea, skin irritation, eye burns and tissue necrosis (PONTES, 2015; ABBAS et al., 2020; PARTILA, 2021).

The other extremely worrying aspect of the constitution of textile industrial effluents is related to color, which is the consequence of the presence of chromophore groups that are part of the structure of dye molecules (CARNEIRO; ZANONI, 2016).

In water bodies, the color given by textile dyes, especially MB, makes it difficult for light to pass through, which significantly affects the performance of photosynthesis by aquatic plants and creates an imbalance in biological cycles (KUNZ, 2002; YU; FENG; YUE, 2015; BHATI et al., 2016).

Given this situation, several methods of physical, biological and chemical water treatment have been developed, tested and employed (KANDELBAUER; CAVACO-PAULO; GÜBITZ, 2007). In practice, however, each one has its advantages and disadvantages (AMOOZEGAR; MEHRSHAD; AKHOONDI, 2015).

From there, it is highlighted that the main objective of this article is to verify the efficiency and influence of pH, photocaliper concentration and aeration on MB heterogeneous photocatalysis.

MATERIALS AND METHODS

Given that reality is not shown on the surface of things, scientific research is required to be equipped with formality, detail and reflection (DEMO, 1985). At the same time, even though it may find partial truths, scientific research has the duty to contribute efficient solutions to everyday problems (MARCONI; LAKATOS, 2003; KALE; JAYANTH, 2019).

One of the strategies used by science is experimental research, which attempts to reproduce, measure or quantify and analyze the phenomena of reality (DEMO, 1985). Therefore, the use of rigorous sampling and data analysis techniques ensures ample space for experimental research, whether in the natural environment or in the laboratory (MARCONI; LAKATOS, 2003).

Regarding experimental laboratory research, it must be said that it represents the best example of scientific investigation, as it allows the environment to be rigorously controlled and the effects associated with the variables of interest to be observed and studied (SOUZA; SANTOS; DIAS, 2013). It is not without reason, then, to state that this type of research proves to be the most appropriate

for the purposes of the present work.

In light of these considerations, it must be noted that the analyte used was MB or methylthioninium chloride (C16H18ClN3S), which has a molar mass of 319.85 g.mol-1 and a structural formula expressed in Figure 1.

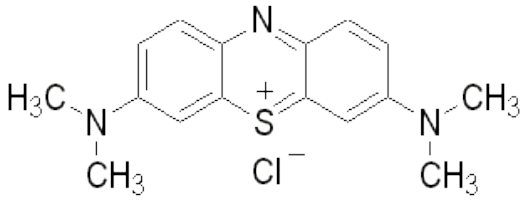

Figure 1. MB structural formula

Source: Prepared by the author

The photocatalyst used was titanium dioxide (TiO2), a 100% anatase mineral variety with a molar mass of 79.866 g.mol-1, produced by IQBC Produtos Químicos Industriais Ltda.

Sulfuric acid (H2SO4), whose molar mass is 98.079 g.mol-1, was, in turn, used to make the necessary pH corrections, drop by drop, until values 3 or 5 were reached, depending on the test. involved. If the value was too low, the pH could be raised using sodium hydroxide (NaOH) with a molar mass of 39.997 g.mol-1. As for pH readings, MQuant Merck test strips were used.

Regarding aeration, the Boyu U-2800 air compressor, 220 V, was used, which was duly equipped with an air outlet or hose. When necessary, due to the test involved, the aforementioned hose was introduced into the glass beaker integral to the reactor.

The experimental apparatus, in turn, included the assembly of a photocatalytic reactor. It consisted of a 250 mL capacity unit, made from a glass beaker, containing a magnetic bar associated with a 220 V voltage magnetic stirrer. A mercury lamp without a bulb, with 125 W of power, was placed 40 cm away from the surface of the solution, present in the photocatalytic reactor, in order to provide UV light.

Since the density of MB is 1 g.mL-1, at 293.15 K or 20ºC, 0.5 mL – equivalent to 0.5 g – was transferred by pipette to a 1 L volumetric flask, the remainder was filled with distilled water in order to obtain a concentration of 500 mg. L-1 for the stock solution. The working solution, in turn, was obtained from 10 mL of the stock solution, which were transferred to a 1 L volumetric flask and filled with distilled water to obtain a concentration of 5 mg. L- 1.

Using a volumetric flask, 200 mL of the MB working solution was transferred to the photocatalytic reactor for each test performed. At the same time, using a 10-4 g precision analytical balance, 0.02 g of TiO2 was weighed in order to obtain tests with a concentration of 0.1 gL-1, while 0.1 g was weighed to perform tests with a concentration of 0.5 gL-1 in the photocatalytic reactor. After the introduction of TiO2, in each test, an attempt was made to homogenize the solution for five minutes using the magnetic bar before turning on the mercury lamp.

Once the mercury lamp was turned on, they waited three minutes for it to fully heat up. In the meantime, 5 mL of the MB solution with TiO2, observing the characteristics of the test, was collected and placed in a glass bottle with a lid, which was labeled with the test order number and the sampling time zero. Then, the glass beaker containing the MB solution with TiO2 was placed below the lamp and the timer was immediately started, so that, every 15 minutes, 5 mL samples were removed from the photocatalytic reactor until the 60-minute limit. Therefore, each sampling was carried out observing t = 0 minutes, t = 15 minutes, t = 30 minutes, t = 45 minutes and t = 60 minutes.

From a wavelength (λ) of 645 nm, the Hach UV spectrophotometer, model DR 3900, was calibrated to obtain data relating to MB absorbances. This way, the 1 cm cuvette of

the spectrophotometer received the aliquots corresponding to the contents of the glass vials. This allowed readings of the respective absorbances to be carried out, which were duly noted and associated with the assay order number and sampling time.

The mathematical basis for the readings taken by the spectrophotometer was expressed by Equation (1):

$$A = \varepsilon . B . w \quad (1)$$

In Equation (1), also known as the Lambert-Beer Law, ε is the molar absorptivity, b is the optical path or thickness of the spectrophotometer cuvette, and c is the analyte concentration. Given that the analyte to be studied is MB at λ = 645 nm, ε = 0.1493 M-1. cm-1 was considered (SAUER; HOFKENS; ENDERLEIN, 2011)

Once the absorbance readings were collected and properly organized, the concentrations were obtained using the essential Lambert-Beer Law.

The determination of MB removal or decolorization rates, in turn, could be achieved using Equation (2):

$$TR = \frac{C_o - C_t}{C_o} . 100\% \quad (2)$$

Using Equation (2), it is observed that Co is the initial concentration and Ct is the MB concentration at a given time t, which were expressed, respectively, in M (ABDELLAH et al., 2018).

Data analysis, in turn, was based on factorial planning 23, that is, on eight trials carried out randomly. This planning basically consisted of two levels of analysis (low and high) accompanied by three factors or variables of interest (pH, TiO2 concentration and aeration). As a result, from the table of contrast coefficients, the complete matrix of contrast coefficients, the transposed matrix and the column vector of the average removal rates, it was possible to determine the effect vector, which supported a robust interpretation analysis of the effects or interactions between levels and factors of interest.

Considering, however, that replications were not used in this experiment, the factorial design 23 could not use analysis of variance or ANOVA.

Alternatively, however, the normal probability graph was used. To this end, the effects were ordered in increasing order. Then, the respective accumulated probabilities expressed by Equation (3) were calculated.

$$P_i = \frac{100.(i-0,5)}{2^k - 1} \quad (3)$$

Note that, in this Equation (3), i represents the increasing order of the effects ek and the number of factors in the factorial planning (CARPINETTI, 2009).

Finally, the normal probability graph was constructed. In it, the accumulated probabilities were represented on the ordinate axis, via a semi-logarithmic scale, while the effect values were projected on the abscissa axis (ARAUJO, 2011). This way, the graphical interpretation of the effects was made possible.

RESULTS AND DISCUSSION

The physical treatments applied to textile industrial effluents, although they act as important forms of pre-treatment and polishing, cannot degrade the dyes, but only transfer them in phase through the formation of sludge. Similarly, biological treatments, although represented by aerated lagoons with low costs and simple operation, do not promote a good removal rate of the color generated by the dyes (BRITO; SILVA, 2012).

It is therefore imperative to use chemical treatment technologies, which are capable of providing the most effective degradation or even mineralization of industrial textile

dyes (KUNZ, 2002; SALLES; PELEGRINI; PELEGRINI, 2006).

Although Fujishima and Honda initially considered the generation of hydrogen (H2) in photocells, heterogeneous photocatalysis must be mentioned, which currently aims to act within the scope of chemical treatments aimed at the degradation or mineralization of inorganic pollutants and organic (JIN-HUI, 2012; GARCÍA-LÓPEZ; MARCÌ; PALMISANO, 2016).

It is an advanced oxidative process capable of producing harmless substances, such as water (H2O) and carbon dioxide (CO2), through the use of radiation or ultraviolet light (UV) and a photocatalyst, which is, as a rule, a metallic oxide (FUJISHIMA; RAO; TRYK, 2000).

The heterogeneous character of the process, in turn, derives from the fact that there is a liquid phase and a solid phase represented by the photocatalyst (MALATO, 2014).

In addition to being relatively cheap and stable, TiO2 acts as an excellent photocaliper or semiconductor, as UV radiation, upon reaching its surface, is capable of exciting or moving the electron from its valence band to its conduction band (SCHNEIDER et al., 2014).

On the other hand, it must be noted that the energy necessary for the excitation or promotion of the electron (hν) must be equal to or greater than the energy of the forbidden or conduction band, which allows the formation of the so-called positive electron-hole pair. (MENDIVE; CURTI; BAHNEMANN, 2016).

The greatest contribution of heterogeneous photocatalysis to the treatment of industrial textile dyes comprises the production of superoxide and hydroxyl radicals. In effect, oxygen, normally dissolved, acts as the receptor for photoexcited electrons, present in the conduction band of TiO2, originating superoxide radicals (FUJISHIMA; RAO; TRYK, 2000).

The positive hole, in turn, formed in the valence band, is capable of directly oxidizing the pollutants themselves or water. In the latter case, hydroxyl radicals considered to be highly reactive are obtained (PARRINO et al., 2021).

According to SCHNEIDER et al. (2014) and PARRINO et al. (2021), Equations (4) to (8) illustrate, in general terms, heterogeneous photocatalysis:

$$TiO2 + h\nu \rightarrow e- + h+ \quad (4)$$

Electron pair e- positive hole h+

$$e- + O2 \rightarrow O2^{\bullet}- \quad (5)$$

Formation of the superoxide radical $O2^{\bullet}-$

$$h+ + pollutant \rightarrow H2O + CO2 \quad (6)$$

Degradation of the pollutant by the positive hole h+

$$h+ + H2O \rightarrow {}^{\bullet}OH + H+ \quad (7)$$

Formation of the hydroxyl radical $^{\bullet}OH$

$$^{\bullet}OH + pollutant \rightarrow H2O + CO2 \quad (8)$$

Degradation of the pollutant by the hydroxyl radical $^{\bullet}OH$

In light of these considerations, the present work set out to investigate whether MB can be removed from water. Therefore, we sought to determine the efficiency and influence of pH, TiO2 concentration and aeration on the heterogeneous photocatalytic degradation of MB.

Factorial planning 23, used here, combines different factors and levels of analysis, which can be duly detailed in Table 1.

In turn, Table 2, presented below, attests that each of the eight tests was carried out randomly, which makes it possible to associate them with the respective Order of Events (OE).

Factors or variables		Levels	
		(-)	(+)
1	pH	3	5
2	[TiO2] [gL-1]	0.1	0.5
3	Aeration	no	Yes

Table 1. Factors and levels of factorial planning 23

Source: Prepared by the author

Essay	Order of Events [OE]	pH	[TiO2] [gL-1]	Aeration
1	5th	3	0.1	no
2	8th	5	0.1	no
3	1st	3	0.5	no
4	7th	5	0.5	no
5	3rd	3	0.1	Yes
6	6th	5	0.1	Yes
7	4th	3	0.5	Yes
8	2nd	5	0.5	Yes

Chart 2. Organization of factorial planning 23

Source: Prepared by the author

Time [minute]	Absorbances [AU]							
	OE 1st	OE 2nd	OE 3rd	OE 4th	OE 5th	OE 6th	OE 7th	OE 8th
0	0.691	0.65	0.735	0.71	0.703	0.693	0.712	0.735
15	0.028	0.141	0.035	0.021	0.064	0.378	0.11	0.302
30	0.006	0.041	0.007	0.008	0.023	0.287	0.055	0.218
45	0.003	0.017	0.007	0.008	0.022	0.162	0.011	0.172
60	0.004	0.02	0.01	0.008	0.014	0.16	0.01	0.130

Table 1. Absorbances as a function of time

Source: Prepared by the author

Furthermore, in each of the columns of the three factors of the factorial design, it becomes clear that the levels oscillate from the lowest to the highest according to the following sequence, namely: 20 out of 20 for pH, 21 out of 21 for the TiO2 concentration and finally 22 in 22 for aeration.

Based on the EO, Table 1 shows the data from the absorbance readings taken from the spectrophotometer.

In turn, Figure 2 provides a graphical visualization of the behavior of MB absorbances.

The decay of MB concentrations, in turn, is numerically represented in Table 2.

Finally, Figure 3 graphically corroborates the aforementioned decline in MB concentrations.

From Figures 2 and 3, it is clearly observed that the absorbances and concentrations of MB decrease as time passes.

At the same time, in most tests, a significant reduction in MB absorbances and concentrations is observed, which already manifests itself in the first 15 minutes and then becomes complete within 60 minutes of photocatalytic activity.

The absorbances and residual concentrations of the 6th and 8th EO, however, stand out for being the highest, as they exhibit the characteristics associated with low photocatalytic activity, namely: [TiO2] = 0.1 gL-1 and the pH = 5, common to both OE, as well as the aeration with bubbles associated with the 6th OE.

The reduction in absorbances and concentrations is understood by the Lambert-Beer Law, as there is a temporal linear relationship between them, or even, absorbances decrease as concentrations decline over time (AARTHI; NARAHARI; MADRAS, 2007; TSENG et al., 2017).

Once the concentrations are found, it is possible to determine the MB removal or decolorization rates (SHEHZAD et al., 2020).

From there, you can also obtain the averages of these rates. Table 3, in this sense, provides the values.

Figure 4, in turn, shows the graphical behavior of removal rates.

It can be seen from Figure 4 that the majority of tests have good MB removal rates in just 15 minutes, while maximum degradation is reached in 60 minutes. The exceptions are, of course, the6th and 8th OE, which exhibit, especially at the end of the photocatalytic process, values below 100% removal. In this sense, the role played by the high pH and low concentration of TiO2, applicable to the case of the 6th and 8th EO, is highlighted, as well as by the aeration with bubbles in the case, specifically, of the6th OE.

Based on the data relating to the factors in Table 2 and the average removal rates in Table 3, the construction of Table 4, which deals with the contrast coefficients, becomes fully viable.

It is observed that the signs of the factors in table 4 are obtained from the content of the pH, TiO2 concentration and aeration columns in table 2, in such a way that the sign (+) relates to the highest level and the (–) at the lowest level found. On the other hand, it must be said that the signs corresponding to the interactions of two and three factors in table 4 are achieved from the multiplication, line by line, of the elements of the appropriate preceding columns (MARINHO; CASTRO, 2005; MONTGOMERY, 2017).

In turn, the identity column of table 4 assumes, by default, values (+). With the exception of it, it appears that the other columns have the same number of positive and negative signs (TOLEDO et al., 2013; MONTGOMERY, 2017).

Lastly, column $\bar{y}$ of table 4 comes from the average MB removal rates provided by table 3 and duly associated with the respective

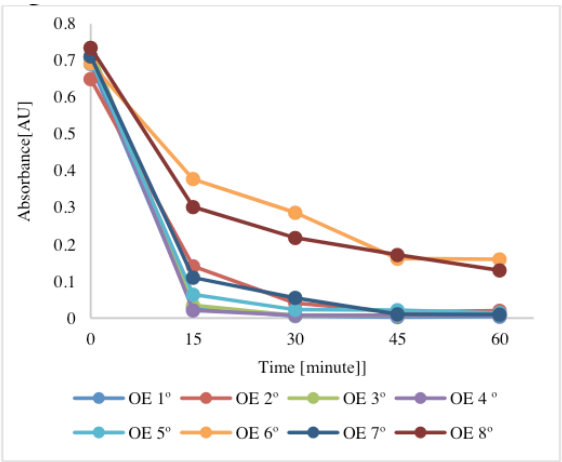

Figure 2. Absorbances as a function of time

Source: Prepared by the author

Time [minute]	Concentrations [M]							
	OE 1st	OE 2nd	OE 3rd	OE 4th	OE 5th	OE 6th	OE 7th	OE 8th
0	4.63	4.35	4.92	4.76	4.71	4.64	4.77	4.92
15	0.19	0.94	0.23	0.14	0.43	2.53	0.74	2.02
30	0.04	0.27	0.05	0.05	0.15	1.92	0.37	1.46
45	0.02	0.11	0.05	0.05	0.15	1.09	0.07	1.15
60	0.03	0.13	0.07	0.05	0.09	1.07	0.07	0.87

Table 2. Concentrations as a function of time

Source: Prepared by the author

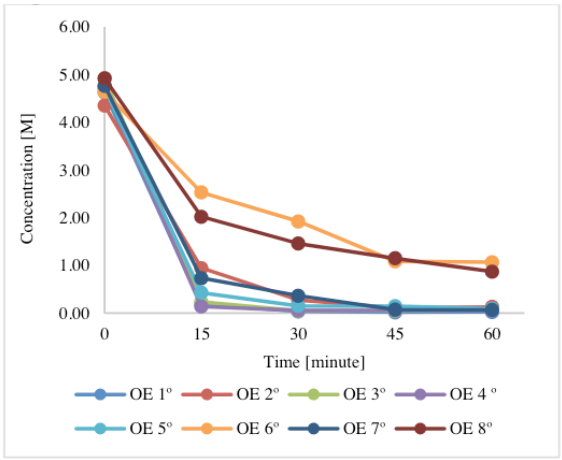

Figure 3. Concentrations as a function of time

Source: Prepared by the author

Time [minute]	Removal rates [%]							
	OE 1st	OE 2nd	OE 3rd	OE 4th	OE 5th	OE 6th	OE 7th	OE 8th
0	0.00	0.00	0.00	0.00	0.00	0.00	0.00	0.00
15	95.95	78.31	95.24	97.04	90.90	45.45	84.55	58.91
30	99.13	93.69	99.05	98.87	96.73	58.59	92.28	70.34
45	99.57	97.38	99.05	98.87	96.87	76.62	98.46	76.60
60	99.42	96.92	98.64	98.87	98.01	76.91	98.60	82.31
Averages	98.52	91.58	97.99	98.42	95.63	64.39	93.47	72.04

Table 3. Removal rates as a function of time and their respective averages

Source: Prepared by the author

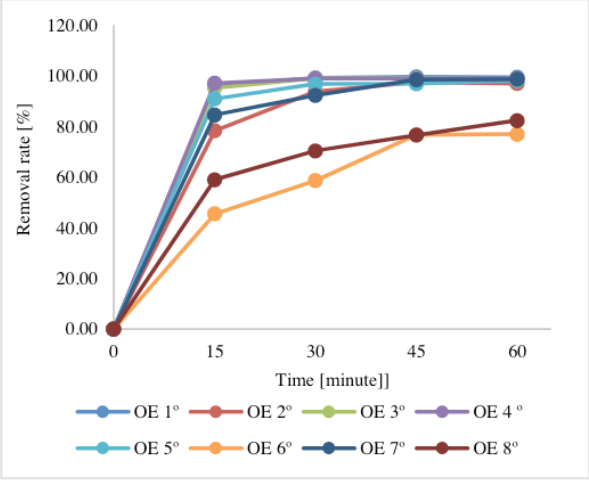

Figure 4. Removal rates

Source: Prepared by the author

Essay	OE	Identity	Factors			Interactions				$\bar{y}$
			1	2	3	12	13	23	123	
1	5th	+	-	-	-	+	+	+	-	95.63
2	8th	+	+	-	-	-	-	+	+	72.04
3	1st	+	-	+	-	-	+	-	+	98.52
4	7th	+	+	+	-	+	-	-	-	93.47
5	3rd	+	-	-	+	+	-	-	+	97.99
6	6th	+	+	-	+	-	+	-	-	64.39
7	4th	+	-	+	+	-	-	+	-	98.42
8	2nd	+	+	+	+	+	+	+	+	91.58

Table 4. Contrast coefficients for factorial planning 23

Source: Prepared by the author

OE. From Table 4, the complete matrix of contrast coefficients (Figure 5) designated as X (BARROS NETO; SCARMINIO; BRUNS, 2010) can be determined.

It becomes evident that the identity column is present in the matrix

The transposed matrix Xt (Figure 6), in turn, arises from the matrix

On the other hand, column $\bar{y}$ of Table 4 of contrast coefficients is transformed into a matrix called column vector $\bar{y}$ (Figure 7), which contains the average MB removal rates proposed by Table 3.

The product between the transposed matrix Xt and the column vector $\bar{y}$ (Figure 8) is shown to be a prerequisite for obtaining the effects involved in this experiment.

Bearing in mind that the result of the matrix product the effects of the factors (pH, TiO2 concentration and aeration) and their respective interactions highlighted in Figure 9 (MARINHO; CASTRO, 2005; BARROS NETO; SCARMINIO; BRUNS, 2010).

It can be seen, then, that factorial planning 23 allows, in addition to the global average, the three main effects to be determined (1, 2, 3) together with the interactions of two factors (12, 13, 23) and three factors (123) (MONTGOMERY, 2017).

The global average, in turn, can be seen as the average of the average MB removal rates. The obtained value of 89.01% must be interpreted as successful.

Effect 1 corresponds to the pH factor and is included in the most significant category in this experiment. In fact, pH is a key factor in photocatalysis, as it is fundamental to the adsorption and degradation of dyes, in addition to interfering with the surface of the TiO2 photocatalyst (THU et al., 2016; KAUR et al., 2018; KHAN, 2018).

According to the second row of the transposed matrixXt, it is observed that the pH factor migrates from the lowest to the highest level, that is, from – 1 to 1. When, then, the pH level transitions from 3 to 5, there is a reduction in the efficiency of MB removal of the order of – 17.27%. In other words, as the pH increases, the photocatalytic efficiency ends up being reduced (EHRAMPOUSH et al., 2011).

On the other hand, according to YU et al. (2007), as the pH decreases from 5 to 3, photocatalytic activity increases. It is worth noting, however, that lower pH values, such as 2, would end up resulting in the transformation of anatase, that is, the most active crystalline structure or phase of TiO2, into rutile, which would imply a reduction in the photocatalysis of TiO2. MB (YU et al., 2007; WELLS, 2009).

One of the causes of the phenomenon that relates pH to photocatalytic efficiency is linked to the size of the crystalline aggregates of the TiO2 photocaliper, which affects its adsorption capacity (CHONG et al. 2010; BEATA et al., 2018). In effect, reducing the pH from 5 to 3 results in a decrease in the crystalline size of TiO2 and, therefore, an increase in its active surface, which results in an increase in MB photocatalysis (YU et al., 2007).

Therefore, in photocatalytic reactions, efficiency is largely influenced by pH (ALKAIM et al., 2013).

Effect 2, in turn, is related to the TiO2 concentration factor and is equivalent to 12.99%. Like effect 1, effect 2 is included in the list of the most significant ones present in this experiment.

The third line of the transposed matrix variation from 0.1 gL-1 to 0.5 gL-1, is responsible for a 12.99% increase in MB removal. It must be noted, however, that increasing the concentration of the photocatalyst can have positive and negative impacts on the photodegradation rate (BANSAL; SUD, 2011).

In this sense, the increase in the amount

$$X = \begin{bmatrix} 1 & -1 & -1 & -1 & 1 & 1 & 1 & -1 \\ 1 & 1 & -1 & -1 & -1 & -1 & 1 & 1 \\ 1 & -1 & 1 & -1 & -1 & 1 & -1 & 1 \\ 1 & 1 & 1 & -1 & 1 & -1 & -1 & -1 \\ 1 & -1 & -1 & 1 & 1 & -1 & -1 & 1 \\ 1 & 1 & -1 & 1 & -1 & 1 & -1 & -1 \\ 1 & -1 & 1 & 1 & -1 & -1 & 1 & -1 \\ 1 & 1 & 1 & 1 & 1 & 1 & 1 & 1 \end{bmatrix}$$

Figure 5. X Matrix

Source: Prepared by the author

$$X^t = \begin{bmatrix} 1 & 1 & 1 & 1 & 1 & 1 & 1 & 1 \\ -1 & 1 & -1 & 1 & -1 & 1 & -1 & 1 \\ -1 & -1 & 1 & 1 & -1 & -1 & 1 & 1 \\ -1 & -1 & -1 & -1 & 1 & 1 & 1 & 1 \\ 1 & -1 & -1 & 1 & 1 & -1 & -1 & 1 \\ 1 & -1 & 1 & -1 & -1 & 1 & -1 & 1 \\ 1 & 1 & -1 & -1 & -1 & -1 & 1 & 1 \\ -1 & 1 & 1 & -1 & 1 & -1 & -1 & 1 \end{bmatrix}$$

Figure 6. Transposed matrix Xt

Source: Prepared by the author

$$\bar{y} = \begin{bmatrix} 95{,}63 \\ 72{,}04 \\ 98{,}52 \\ 93{,}47 \\ 97{,}99 \\ 64{,}39 \\ 98{,}42 \\ 91{,}58 \end{bmatrix}$$

Figure 7. Column vector $\bar{y}$

Source: Prepared by the author

$$X^t.\bar{y} = \begin{bmatrix} 712{,}04 \\ -69{,}08 \\ 51{,}94 \\ -7{,}28 \\ 45{,}3 \\ -11{,}8 \\ 3{,}3 \\ 8{,}22 \end{bmatrix}$$

Figure 8. Matrix product $X^t.\bar{y}$

Source: Prepared by the author

$$\begin{bmatrix} \text{Average} \\ 1 \\ 2 \\ 3 \\ 12 \\ 13 \\ 23 \\ 123 \end{bmatrix} = \begin{bmatrix} 89{,}01 \\ -17{,}27 \\ 12{,}99 \\ -1{,}82 \\ 11{,}33 \\ -2{,}95 \\ 0{,}83 \\ 2{,}06 \end{bmatrix}$$

Figure 9. Global average associated with the vector of factor effects

Source: Prepared by the author

of photocaliper is related to the expansion of the total active surface area, which provides an increase in the number of •OH and O2•- radicals (LIMA et al., 2014; ABDELLAH et al., 2018).

On the other hand, high concentrations of TiO2 can cause an increase in the turbidity of the solution, a reduction in the passage of UV light and, consequently, a decrease in photocatalytic activity, in addition to being economically unviable in large-scale operations (DANESHVAR; SALARI; KHATAEE, 2004).

Either way, it becomes clear that the photocatalytic efficiency is substantially influenced by the TiO2 concentration (ABDELLAH et al., 2018).

On your turn, effect 3 is linked to the aeration factor. Unlike precedents 1 and 2, effect 3 is included in the scope of effects of lesser influence or efficiency.

The fourth line of the transposed matrix If it goes from the absence to the presence of aeration, effect 3 promotes a reduction of – 1.82% in the MB removal efficiency.

It is known that, during photocatalysis, dissolved oxygen is the acceptor of excited electrons resulting from the TiO2 conduction band (TUNG; ANANPATTARACHAI; KAJITVICHYANUKUL, 2018).

This photocatalytic mechanism originates O2•- radicals that can degrade organic pollutants, such as MB (PRATAMA; ARTSANTI, 2019).

Molecular water itself can react with the protonated or positive h+ holes of the TiO2 valence band and produce •OH radicals (JAWAD et al., 2016).

Another possibility involves the degradation of MB through holes in the valence band of TiO2 without the intermediation of radicals (SALGADO; VALENTINI, 2019).

However, a high aeration rate can cause the formation of a large number of bubbles, a reduction in the passage of UV light and, consequently, a decrease in photocatalytic efficiency (NAWAWI et al., 2017).

This phenomenon, without a doubt, can be applied here, since the aeration used used an air compressor without greater control over the flow. Furthermore, the dissolved oxygen content itself, provided by mechanical aeration, may not have been sufficient, as atmospheric air only contains 21% of this gas. In these circumstances, then, it must be said that aeration ended up not offering the expected result for photocatalytic efficiency.

Effect 12, in turn, stands out among the interaction effects of two and three factors, as it favors an increase of 11.33% in MB degradation. Therefore, effect 12 is included among the most significant effects. This is due to the fact that it is the result of the combination between pH and TiO2 concentration. Therefore, its action is associated both with the increase in the active surface of the photocatalyst and with the generation of radicals •OH and O2•- that act in the degradation of MB.

Effect 13 comes from the interaction between pH and aeration. In this case, although pH is an important factor for the expansion of the TiO2 active surface, the action of bubbles arising from compressor aeration may have attenuated the transmission of UV light. As a result, the degree of MB removal ended up being reduced to – 2.95%, which makes it possible to associate effect 13 with the set of effects of lesser significance or efficiency.

Analogously to effect 13, it can be said that in the case of effect 23, although the concentration of the photocaliper may be associated with the action of radicals •OH and O2•-, the influence of aeration bubbles was present again, in order to unbalance the interaction and thus reduce the photocatalytic efficiency. Thus, effect 23 only contributes 0.83% to the removal of MB, which makes

it possible to classify it within the scope of effects of lesser influence or efficiency.

Finally, the effect 123 is composed of the interaction of the three factors adopted in the factorial design 23, namely, pH, TiO2 concentration and aeration. In this effect, although there is a role played by the active surface of the photocatalyst, combined with the action of the •OH and O2•- radicals, it is understood that the action of the aeration bubbles attenuated the passage of UV light and proved, once again, strongly active. As a result, effect 123 provides a modest level of MB removal of 2.06%, which places it in the category of effects of lesser importance or efficiency (Table 5).

Figure 10, in turn, provides the graphical form of the normal probability in order to ensure a better characterization or visualization of the effects and their respective interactions. To do so, it uses table 5, which displays the increasing ordering of the effects and their accumulated probabilities.

When taking the vertical axis centered at zero as a reference, it can be seen in Figure 10 that the points of least influence or efficiency in this experiment can be grouped around a straight line that crosses this axis (CARPINETTI, 2009).

Such points comprise precisely the interactions where aeration, that is, effect 3 (– 1.82) is present, that is, the interactions of two factors 13 (– 2.95) and 23 (0.83) and three factors 123 (2.06), which exhibit the lowest photocatalytic efficiencies.

On the other hand, the points and, consequently, the effects furthest from this vertical axis are the most significant (ARAUJO, 2011). Therefore, it can be seen in Figure 10 that, regardless of the signs, the most important effects in this experiment are represented by pH and TiO2 concentration, that is, by effects 1 (– 17.27) and 2 (12.99), as well as its corresponding interaction 12 (11,33).

It becomes evident, then, that factorial planning 23 and the normal probability graph are powerful tools capable of analyzing several factors and levels at the same time, in such a way that the responses or effects achieved can be interpreted for the benefit of improving the experiment carried out (CALEGARE, 2009; NÓBREGA, 2010).

CONCLUSION

The present work therefore proposed to verify the efficiency and influence of pH, TiO2 concentration and aeration on MB heterogeneous photocatalysis.

The 23 factorial design and the normal probability graph allowed, in this experiment, not only the determination of the effects, but also their visualization or graphic interpretation. This way, it was possible to assess the effects of greater and lesser influence and efficiency for the degradation or removal of MB from water.

When the pH increases from 3 to 5, there is a decrease of – 17.27% in photocatalysis. As a result, it can be said that the reverse process of reducing the pH from 5 to 3 tends to increase the photocatalytic efficiency, since the active surface of the TiO2 crystals is enlarged. It must be noted, however, that pH values lower than 3 are not interesting due to the transformation of TiO2 from the anatase phase to rutile, which appears to be less efficient from a photocatalytic point of view.

As for the TiO2 concentration, it is observed that the increase from 0.1 gL-1 to 0.5 gL-1 is associated with a 12.99% increase in photocatalytic efficiency. It is believed that the main reason for this phenomenon is linked to the growth of the total active surface area of the photocatalyst, in such a way that thenumber of radicals •OH and O2•- increases in favor of photocatalysis. On the other hand, it must be noted that high concentrations of TiO2 tend

i	Effects	Cumulative probability
1	-17.27	7.1
2	-2.95	21.4
3	-1.82	35.7
4	0.83	50
5	2.06	64.3
6	11.33	78.6
7	12.99	92.9

Table 5. Cumulative probability of effects

Source: Prepared by the author

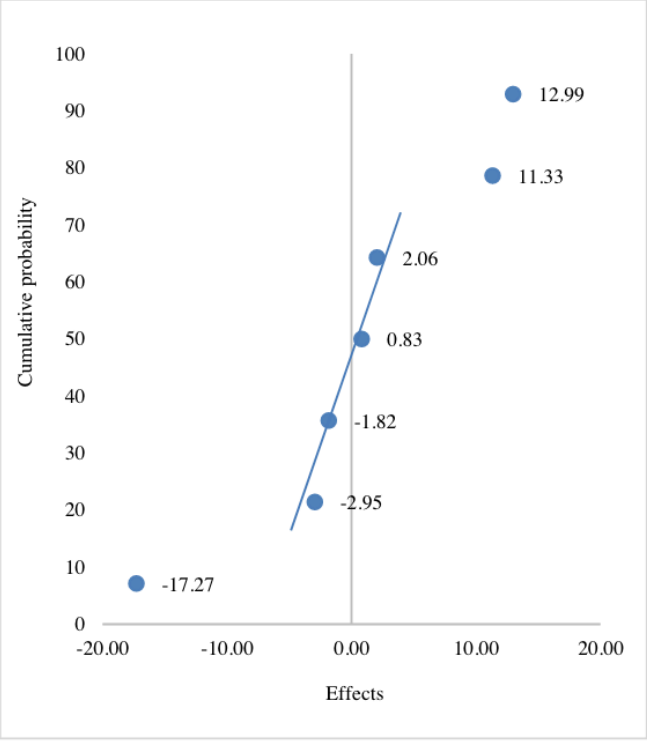

Figure 10. Normal probability of effects

Source: Prepared by the author

to generate turbidity, a decrease in the passage of UV light and a reduction in photocatalytic activity, as well as increasing the cost of treatment in large-scale projects.

Regarding aeration, it is noted that its presence generates a reduction of – 1.82% in photocatalytic efficiency. This can be attributed both to the fact that mechanical aeration produces low levels of dissolved oxygen in the water, and to the fact that it induces, due to the equipment used, the substantial formation of bubbles that reduce the action of UV light. As a result, in all interactions of factors where it was shown to be active, aeration is attested to the occurrence of lower efficiency results or influence on the photocatalytic degradation of MB.

In any case, it must be said that the heterogeneous photocatalysis, promoted by the use of UV light and the semiconductor TiO2, made it possible, in this experiment, for the MB textile dye to be successfully degraded from water, since an average overall 89.01%. At the same time, it is imperative to point out that the factors with the greatest influence and efficiency, relating to the experimental conditions developed here, include pH = 3 and [TiO2] = 0.5 gL-1, as well as their respective interaction or arrangement.

Although aeration has been used with the aim of achieving a more economical generation of oxygen, it is suggested, for future research, that the effect associated with increasing the content of pure oxygen dissolved in water be investigated. It is believed, in this sense, that the increase in the supply of pure dissolved oxygen will tend to facilitate the process of reduction in oxygen.the TiO2 conduction band and, consequently, enable the formation of $O_2^{\bullet-}$ radicals.

At the same time, it is proposed to replace the air compressor with better equipment, which may be capable of ensuring greater control of the gas flow and, thus, reducing or avoiding excessive bubble formation.

Finally, another suggestion for improvement for future work concerns the prospecting for a borderline concentration of TiO2, which could act as an optimal point between maximum photocatalytic efficiency and economic rationalization of the MB photocatalysis process.

REFERENCES

AARTHI, T.; NARAHARI, P.; MADRAS, G. Photocatalytic degradation of Azure and Sudan dyes using nano TiO_2. **Journal of Hazardous Materials**, Amsterdam, v. 149, n. 3, p. 725-734. 2007.

ABBAS, H. A. et al. Photocatalytic degradation of Methylene Blue dye by fluorite type $Fe_2Zr_{2-x}W_xO_7$ system under visible light irradiation. **Ecotoxicology and Environmental Safety**, Cambridge, v. 196, n. 1, p. 1-10. 2020.

ABDELLAH, M. H. et al. Photocatalytic decolorization of Methylene Blue using TiO_2/UV system enhanced by air sparging. **Alexandria Engineering Journal**, Alexandria, v. 57, n. 4, p. 3727-3735. 2018.

AGARWAL, S. K. **Water pollution**. New Delhi: APH Publishing, 2009. 384 p.

ALKAIM, A. F. et al. Enhancing the photocatalytic activity of TiO_2 by pH-control: a case study for the degradation of EDTA. **Catalysis Science & Technology**, Zurich, v. 3, n. 12, p. 1-6. 2013.

AMOOZEGAR, M. A.; MEHRSHAD, M.; AKHOONDI, H. Application of extremophilic microorganisms in decolorization and biodegradation of textile wastewater. In: SINGH, S. N. (Ed.). **Microbial degradation of synthetic dyes in wastewaters**. Berlin: Springer, 2015. p. 267-296.

ARAUJO, F. V. F.; YOKOYAMA, L.; TEIXEIRA, L. A. C. Remoção de cor em soluções de corantes reativos por oxidação com H_2O_2/UV. **Química Nova**, São Paulo, v. 29, n. 1, p. 11-14. 2006.

ARAUJO, J. P. D. **A aplicação de planejamento estatístico multivariado no desenvolvimento de componentes do motor diesel**. 2011. 85 f. Dissertação (Mestrado em Engenharia Automobilística) – Faculdade de Engenharia Mecânica, Universidade Estadual de Campinas, Campinas, 2011.

BANSAL, P.; SUD, D. Photodegradation of commercial dye Procion Blue HERD. **Desalination**, Swansea, v. 267, n. 2, p. 244-249. 2011.

BARROS NETO, B.; SCARMINIO, I. S.; BRUNS, R. E. **Como fazer experimentos**: pesquisa e desenvolvimento na ciência e na indústria. 4. ed. Porto Alegre: Bookman, 2010. 413 p.

BEATA, B. et al. Application of metal oxide-based photocatalysis. In: ZALESKA-MEDYNSKA, A. (Ed.). **Metal oxide-based photocatalysis**. Amsterdam: Elsevier, 2018. p. 211-340.

BHATIA, S. C. **Pollution control in textile industry**. London: CRC Press, 2017. 342 p.

BHATI, A. et al. Sunlight-induced photochemical degradation of Methylene Blue by water soluble carbon nanorods. **International Journal of Photoenergy**, London, v. 4, n. 1, p. 1-9. 2016.

BRITO, N. N.; SILVA, V. B. M. Processo oxidativo avançado e sua aplicação ambiental. **Revista Eletrônica de Engenharia Civil**, Goiânia, v. 3, n. 1, p. 36-47. 2012.

CALEGARE, A. J. A. **Introdução ao delineamento de experimentos**. 2. ed. rev. e atual. São Paulo: Blücher, 2009. 145 p.

CARNEIRO, P. A.; ZANONI, M. V. B. Corantes têxteis. In: ZANONI, M. V. B.; YAMANAKA, H. (Orgs.). **Corantes**: caracterização química, toxicológica, métodos de detecção e tratamento. São Paulo: Editora Unesp, 2016. p. 13-35.

CARPINETTI, L. C. R. **Planejamento e análise de experimentos**. São Carlos: USP, 2009. 222 p. Material de curso.

CHONG, M. N. et al. Recent developments in photocatalytic water treatment technology: review. **Water Research**, London, v. 44, n. 10, p. 2997-3027. 2010.

DANESHVAR, N.; SALARI, D.; KHATAEE, A. R. Photocatalytic degradation of azo dye Acid Red 14 in water on ZnO as an alternative catalyst to TiO_2. **Journal of Photochemistry and photobiology**, Lausanne, v. 162, n. 2, p. 317-322. 2004.

DEMO, P. **Introdução à metodologia da ciência**. 2. ed. São Paulo: Atlas, 1985. 122 p.

EHRAMPOUSH, M. H. et al. Removal of Methylene Blue dye from textile simulated sample using tubular reactor and TiO_2/UV-C photocatalytic process. **Iranian Journal of Environmental Health Science and Engineering**, Tehran, v. 8, n. 1, p. 35-40. 2011.

FUJISHIMA, A.; RAO, T. N.; TRYK, D. A. Titanium dioxide photocatalysis. **Journal of Photochemistry and Photobiology C**, Amsterdam, v. 1, n. 1, p. 1-21. 2000.

GARCÍA-LÓPEZ, E. I.; MARCÌ, G.; PALMISANO, L. Heteropolyacid-based heterogeneous photocatalysts for environmental application. In: COLMENARES, J. C.; XU, Y. (Eds.). **Heterogeneous photocatalysis**. Berlin: Springer, 2016. p. 63-108.

GREGORY, P. Toxicology of textile dyes. In: CHRISTIE, R. M. (Ed.). **Environmental aspects of textile dyeing**. Sawston: Woodhead Publishing Limited, 2007. p. 44-73.

HORNE, A. C. et al. **Water for the environment**. Amsterdam: Elsevier; Cambridge: Academic Press, 2017. 758 p.

JAWAD, A. H. et al. Kinetics of photocatalytic decolorization of cationic dye using porous TiO_2 film. **Journal of Taibah University for Science**, Medina, v. 44, n. 3, p. 352-362. 2016.

JIN-HUI, Z. Research on UV/TiO_2 photocatalytic oxidation of organic matter in drinking water and its influencing factors. **Procedia Environmental Sciences**, Amsterdam, v. 12, n. 1, p. 445-452. 2012.

KALE, G. V.; JAYANTH, J. Introduction to research. In: BAIRAGI, V.; MUNOT, M. V. (Eds.). **Research methodology**: a practical and scientific approach. Boca Raton: CRC Press, 2019. p. 1-24.

KANDELBAUER, A.; CAVACO-PAULO, A.; GÜBITZ, G. Biotechnological treatment of textile dye effluent. In: CHRISTIE, R. M. (Ed.). **Environmental aspects of textile dyeing**. Sawston: Woodhead Publishing Limited, 2007. p. 212-224.

KANT, R. Textile dyeing industry: an environmental hazard. **Natural Science**, Wuhan, v. 4, n. 1, p. 22-26. 2012.

KAUR, H. et al. Role of pH on the photocatalytic activity of TiO2 tailored by W/T mole ratio. **Journal of Materials Science**, Berlin, v. 29, n. 7, p. 1-16. 2018.

KHAN, M. M. Metal oxide powder photocatalysts. In: LIN, Z.; YE, M.; WANG, M. **Multifunctional photocatalytic materials for energy**. Sawston: Woodhead Publishing Limited, 2018. p. 5-17.

KUNZ, A. et al. Novas tendências no tratamento de efluentes têxteis. **Química Nova**, São Paulo, v. 25, n. 1, p. 78-82. 2002.

LANGMUIR, C. H.; BROECKER, W. **How to build a habitable planet**. Princeton: Princeton University Press, 2012. 718 p.

LIMA, G. G. C. et al. Estudo comparativo da aplicação de nanopartículas de TiO_2 e ZnO na descoloração fotocatalítica de uma solução de corante empregando radiação UV artificial. **Revista Eletrônica de Materiais e Processos**, Campina Grande, v. 9, n. 1, p. 22-27. 2014.

MALATO, S. et al. Decontamination of water by solar irradiation. In: LITTER, M. I. (Ed.). **Advanced oxidation technologies**. Boca Raton: CRC Press, 2014. v. 9, p. 1-22.

MARCONI, M. A.; LAKATOS, M. **Fundamentos de metodologia científica**. 5. ed. São Paulo: Atlas, 2003. 310 p.

MARINHO, M. R. M.; CASTRO, W. B. Planejamento fatorial: uma ferramenta poderosa para os pesquisadores. In: CONGRESSO BRASILEIRO DE ENSINO DE ENGENHARIA, 33., 2005, Campina Grande. **Anais...** Campina Grande: COBENGE, 2005. p. 1-10.

MENDIVE, C. B.; CURTI, M.; BAHNEMANN, D. Current issues concerning the mechanism of pristine TiO_2 photocatalysis and the effects on photonic crystal nanostructures. In: SCHNEIDER, J. et al. (Eds.). **Photocatalysis**. London: Royal Society of Chemistry, 2016. p. 51-79.

MONTGOMERY, D. C. **Introdução ao controle estatístico da qualidade**. 7. ed. Rio de Janeiro: LTC, 2017. 544 p.

NAWAWI, W. I. et al. Immobilized TiO_2 Polyethylene-Glycol: effects of aeration and pH of Methylene Blue dye. **Applied Sciences**, Basel, v. 7, n. 5, p. 1-10. 2017.

NÓBREGA, M. P. **Estudo comparativo de gráficos de probabilidade normal para análise de experimentos fatoriais não replicados**. 2010. 182 f. Dissertação (Mestrado em Matemática Aplicada e Estatística) – Centro de Ciências Exatas e da Terra, Universidade Federal do Rio Grande do Norte, Natal, 2010.

PARRINO, F. et al. Properties of titanium dioxide. In: _____; PALMISANO, L. (Eds.). **Titanium dioxide (TiO_2) and its applications**. Amsterdam: Elsevier, 2021. p. 13-66.

PARTILA, A. M. Effect of microbially produced silver nanoparticles on bioremediation of waste dye. In: ADETUNJI, C. O.; PANPATTE, D. G.; JHALA, Y. K. (Eds.). **Microbial rejuvenation of polluted environment**. Berlin: Springer, 2021. v. 3, p. 161-185.

PATEL, H.; VASHI, R. T. **Characterization and treatment of textile wastewater**. Amsterdam: Elsevier; Oxford: Butterworth-Heinemann, 2015. 174 p.

PONTES, J. P. S. D. **Avaliação do tratamento eletroquímico (direto e indireto) como alternativa de degradação do corante azul de metileno**. 2015. 114 f. Tese (Doutorado em Química) – Instituto de Química, Universidade Federal do Rio Grande do Norte, Natal, 2015.

PRATAMA, N. A.; ARTSANTI, P. Effect of aeration treatment on Methylene Blue removal using TiO_2 zeolite. In: INTERNATIONAL CONFERENCE ON SCIENCE AND ENGINEERING, 3rd, 2019, Kuala Lumpur. **Proceedings…** Kuala Lumpur: ICSE, 2019. p. 219-224.

ROBINSON, G. W. et al. **Water in biology, chemistry and physics**. London: World Scientific, 1996. 509 p.
SALGADO, B. C. B.; VALENTINI, A. Evaluation of the photocatalytic activity of SiO_2 and TiO_2 hybrid spheres in the degradation of Methylene Blue and hydroxylation of benzene: kinetic and mechanistic study. **Brazilian Journal of Chemical Engineering**, São Paulo, v. 36, n. 4, p. 1501-1518. 2019.

SALLES, P. T. F.; PELEGRINI, N. N. B.; PELEGRINI, R. T. Tratamento eletroquímico de efluente industrial contendo corantes reativos. **Engenharia Ambiental**, Espírito Santo do Pinhal, v. 3, n. 2, p. 25-40, jul./dez. 2006.

SAUER, M.; HOFKENS, J.; ENDERLEIN, J. **Handbook of fluorescence spectroscopy and imaging**. Weinheim: Wiley-VCH, 2011. 290 p.

SCHNEIDER, J. et al. Understanding TiO_2 photocatalysis: mechanisms and materials. **Chemical Reviews**, Chicago, v. 114, n. 19, p. 9919-9986. 2014.

SENGUPTA, P. K. **Industrial water resource management**: challenges and opportunities for corporate water stewardship. Hoboken: John Wiley & Sons, 2018. 488 p.

SHAMMAS, N. K.; WANG, L. K. **Water and wastewater engineering**. 3rd ed. Hoboken: John Wiley & Sons, 2011. 864 p.

SHEHZAD, N. et al. Development of $AgFeO_2$/rGO/TiO2 ternary composite photocatalysts for enhanced photocatalytic dye decolorization. **Crystals**, Basel, v. 10, n. 923, p. 1-15. 2020.

SOUZA, G. S.; SANTOS, A. R.; DIAS, V. B. **Metodologia da pesquisa científica**. Porto Alegre: Editora Animal, 2013. 164 p.
THU, T. N. T. et al. Synthesis, characterization and effect of pH on degradation of dyes of copper-doped TiO_2. **Journal of Experimental Nanoscience**, London, v. 11, n. 3, p. 226-238. 2016.

TOLEDO, J. C. et al. **Qualidade**: gestão e métodos. Rio de Janeiro: LTC, 2013. 397 p.

TSENG, H. et al. A study of photocatalysis of Methylene Blue of TiO_2 fabricated by electric spark discharge method. **Journal of Nanomaterials**, London, v. 2017, n. 1, p. 1-8. 2017.

TUNG, T. V.; ANANPATTARACHAI, J.; KAJITVICHYANUKUL, P. Photocatalytic membrane reactors for water and wastewater treatment applications: process factors and operating conditions review. **Lowland Technology International Journal**, Saga, v. 20, n. 3, p. 413-424. 2018.

VARANDANI, N. S. **Environmental engineering**: principles and practices. London: Pearson, 2017. v. 1, 593 p.

VON SPERLING, M. **Introdução à qualidade das águas e ao tratamento de esgotos**. 3. ed. Belo Horizonte: Editora UFMG, 2005. 243 p.

WELLS, R. P. K. Oxide materials in photocatalytic process. In: JACKSON, S. D.; HARGREAVES, J. S. J. **Metal oxide catalysis**. Weinheim: Wiley-VCH, 2009. v. 2, p. 755-770.

YU, H. et al. Preparation of nitrogen-doped TiO_2 nanoparticle catalyst and its catalytic effect activity under visible light. **Chinese Journal of Chemical Engineering**, Beijing, v. 15, n. 6, p. 802-807. 2007.

YU, X. Z.; FENG, Y. X.; YUE, D. M. Phytotoxicity of Methylene Blue to rice seedlings. **Global Journal of Environmental Science and Management**, Tehran, v. 1, n. 3, p. 199-204. 2015.